Optical Study of the Strain-driven Tuning of the Emission Energy in InAs/InGaAs Quantum Dot Nanostructures

M. Geddo[1], G. Guizzetti[2], V. Bellani[2], M. Patrini[2], T. Ciabattoni[2], L. Seravalli[3], P. Frigeri[3], M. Minelli[3] and S. Franchi[3]

[1]INFM -UdR Pavia and Dipartimento di Fisica dell' Università di Parma, Parco delle Scienze 7a, I-43100 Parma, Italy
[2]INFM and Dipartimento di Fisica "A. Volta" dell' Università di Pavia, Via Bassi 6, I-27100 Pavia, Italy
[3]CNR-IMEM Institute, Parco delle Scienze 37a, I-43100 Parma, Italy

ABSTRACT

We report on photoreflectance (PR) measurements in the 0.8-1.5 eV photon energy range and at temperatures from 80 to 300 K of InAs self-assembled quantum dots (QDs) grown by Atomic-Layer Molecular Beam Epitaxy. The QDs are embedded in a $In_{0.15}Ga_{0.85}As$ lower confining layer (LCL) with thickness ranging from 20 to 360 nm and in a 20 nm thick upper confining layer with the same composition, that we assume to be pseudomorphic to the LCL. The structures were previously characterized by spectroscopic ellipsometry, photo-luminescence and atomic force microscopy. PR spectra show clear and well-resolved spectral features due to both the QD ground-state transitions and the interband transitions between the topmost split valence bands and the lowest conduction band of LCLs. This allows to self-consistently study the effects on the QD emission energy of parameters such as thickness and composition of partially-relaxed LCLs, that determine the QD strain amount and the QD-CL band discontinuities. In this work, these two contributions to the tuning of the QD emission energy are separated by comparing experimental results to that calculated by means of a simple and yet valuable model for ground-state transitions in QDs. It is proved that QD strain (related to the CL-QD lattice-mismatch determined by the thickness-dependent LCL strain-relaxation) can be effectively used to tune the QD emission energy at room-temperature, in particular in the 1.3 μm window.

I. INTRODUCTION

The tunability of quantum dots (QDs) properties [1] and, above all, of their characteristic emission energy have significantly widened the application field of nanostructures. In particular, concerning silica fiber optic communication, it has been recently shown [2] that by using $In_xGa_{1-x}As$ confining layers, InAs QDs grown by Atomic Layer Molecular Beam Epitaxy (ALMBE) efficiently emitting at 1.3 μm at room temperature can be prepared. Moreover, by controlling the QD strain by means of a suitable choice of thickness and composition of the lower confining layer (LCL), emission wavelengths well beyond 1.55 μm could be obtained, if the emission were not thermally quenched [2].

In the last years different explanations have been presented for the tuning mechanism which controls the red-shift of the emission energy in InAs/InGaAs nanostructures, as compared to that of the InAs/GaAs ones. Among them. two limiting cases may be selected: according to Ustinov *et al.* [3,4] the red-shift is mainly related to the reduction of the band discontinuities in InAs/InGaAs structures, which, in turn, causes the reduction of the confinement energies of carriers. On the other hand, according to Nishi *et al.* [5] the red-shift is due to the decrease of the strain field of InAs dots embedded in InGaAs confining layers, that results in a smaller value of the energy gap of the QD material.

To date, the separation of the effects of confining layers in lowering the band discontinuities and in reducing the strain of QDs is an interesting topic that should be clarified in order to properly engineer the emission energy of the nanostructures.

Here we present systematic photoreflectance (PR) measurements on $InAs/In_xGa_{1-x}As$ QDs with x=0.15, grown by ALMBE. The sample structure was designed so as to control the thickness-dependent strain relaxation of lower confining layers (LCL) on which the QDs are deposited and, in turn, the lattice mismatch between LCLs and QDs, that determines the strain of QDs [2].

Taking advantage of the derivative-like nature and the high room temperature performance of PR spectroscopy, signals coming from different depths of the samples were detected, allowing the unambiguous assignment of the spectral features to bulk- and QD- related transitions. The features of the PR spectra were analyzed according to the lineshape model characteristic of modulation spectroscopy in bulk [10] and confined [11,12] semiconductor systems. The simultaneous determination of the energies of the QD ground-state critical point (CP), of the fundamental band gap and of the valence band splitting of the partially relaxed InGaAs CLs, leads to a valuable correlation of barrier discontinuities and QD strain with the QD emission energies. This is substantiated by the comparison between experimental results and those calculated by means of a model that can be used to engineer the structures.

II. EXPERIMENTAL DETAILS

The sample structure was designed taking into account that InGaAs LCLs are lattice-mismatched to the GaAs substrates and, then, have residual strain that depend on their thickness. According to the Marée *et al.* theory on strain

relaxation of a mismatched layer over a substrate [13], for layer thickness t larger than the critical thickness t_c for strain relaxation the in-plane component of the residual strain ε_{res} of the mismatched layer is given by: $\varepsilon_{res} = \varepsilon_o (t_c / t)^{1/2}$, where ε_o is the lattice mismatch of the involved materials. Therefore, by means of the thickness-dependent residual strain of LCLs, we are able to control the strain imposed to QDs, since the strain is completely determined by the mismatch between QDs and LCLs, for given QD shapes, sizes and compositions [1].

The structures consist of: 1) a 100 nm thick GaAs buffer layer grown by MBE on a (100) GaAs substrate, 2) a $In_{0.15}Ga_{0.85}As$ LCL of thickness t (20 nm < t < 360 nm) grown by MBE at 490 °C, 3) a plane of InAs QDs with a 3 ML coverage deposited by ALMBE at 460 °C, and 4) a 20 nm thick $In_{0.15}Ga_{0.85}As$ upper confining layer (UCL), grown by ALMBE at low temperature (360 °C) in order to reduce the interaction between confining layers and QDs. In some cases, identical structures without UCLs are grown. Further details about growth conditions of the structures and about the ALMBE technique may be found in Refs. [2,14,15].

We assume that the UCLs are pseudomorphic to the LCLs and, then, that the mismatch between UCLs and QDs equals that between LCLs and QDs. This assumption: *i)* is reasonable since the UCL thicknesses are smaller than the critical thicknesses for all the structures [2] and *ii*) will be experimentally justified below.

The mean sizes of QDs were determined by Atomic Force Microscopy in contact-mode on structures without UCLs; base diameters and heights of 21 nm and 4 nm, respectively, were measured, that are independent on LCL thicknesses and, then, on QD strain; the diameter values were corrected by taking into account the convolution between QDs and probe-tip.

The samples were previously studied by photoluminescence [2] and the results showed that, for a CL composition of x = 0.15 and for LCL thickness slightly exceeding t_c the RT QD emission wavelengths are within the 1.3 μm spectral window of optoelectronic interest.

The strain status of the InGaAs CLs was evidenced through the energy and lineshape of E_1 and $E_1 + \Delta_1$ interband critical points in the dielectric functions derived by spectroscopic ellipsometry (SE). Ellipsometric functions were taken at room temperature in the 1.4-5 eV range using a rotating polarizer ellipsometer SOPRA ES4G at two angles of incidence 70° and 75° on pairs of samples with and without the UCLs.

PR measurements were performed at near-normal incidence in the 0.8-1.5 eV range, with energy step and spectral resolution of 1 meV. The standard experimental apparatus operates with a 100 W halogen lamp as probe source. The excitation source is provided by a 16 mW He-Ne laser, mechanically chopped at a frequency of 220 Hz. The sample is mounted in thermal contact with the cold finger of a micro-miniature Joule-Thompson refrigerator coupled with a programmable temperature controller that allows measurements in the 80-300 K temperature range.

The experimental results on the energies of QD ground-state transitions have been compared to the results [2] of a model developed under single-band, effective-mass approximation [16]. The QDs have been considered with: *i)* a cylindrical symmetry, *ii)* a composition equal to the nominal one, *iii)* sizes determined by AFM studies and *iv)* shapes of a truncated cone with R/r = 2.5, where R and r are the major and minor radii. The strain in the QDs (proportional to the QD-LCL mismatch) is taken from the analytical treatment of Andreev *et al.* [17].

III. DATA REDUCTION AND ANALYSIS

The analysis of the PR spectra was carried out by using typical lineshape models characterizing electromodulated signals in semiconductor systems; signals coming from different depths of samples are distinguished and interpreted according to the Aspnes treatment [10]. It has been proved that the PR signal mainly arises from the periodic pump-beam modulation of the surface built-in electric field: when the laser is on, photoexcited carriers partially neutralize surface state charges, driving the native field towards the flat bands condition. Aspnes showed that in the low-field limit (this is usually the case for PR, if Franz-Keldysh oscillations are absent) and near a critical point (CP) the modulated reflectance signal $\Delta R/R$ in bulk semiconductors is characterized by the third-derivative-like behavior of the lineshape and may be expressed by:

$$\Delta R/R = \mathrm{Re}\left[C\, e^{i\varphi}\, (E - Ec + i\Gamma)^{-n}\right] \qquad (1)$$

where E is the energy of the probe beam, C and φ are an amplitude and a phase factor that vary slowly with E, Ec is the CP energy, Γ is the (lorentzian) broadening parameter for Ec and n is an integer or half-integer depending on the CP type (n=2.5 for a three-dimensional CP).

On the other hand, it has been proved that in quantum-sized structures PR is a first-derivative spectroscopy [11]. In particular, for a quantum-confined transition in a single quantum well (QW) it has been shown [11,12] that the first-derivative functional form describing the electromodulated reflectance is formally the same as in Eq. (1) with n=3 (excitonic transition). Following Aigouy *et al.* [18] we used this functional form, which satisfactorily reproduces the 1st derivative of a gaussian profile for the dielectric function, taking into account the inhomogeneous broadening related to size and thickness fluctuations of QDs and QWs, respectively. The gaussian lineshape model was already successfully applied to electroreflectance and PR spectra of QWs [11,12,19], QDs and stacked planes of QDs. [18, 20, 21]. Therefore, we assumed a 3rd derivative behavior (with n = 2.5 in Eq.(1)) when performing fits to the PR structures relative to InGaAs CLs and a 1st derivative behavior (with n=3) in the case of ground-state QD excitonic transitions.

IV. RESULTS AND DISCUSSION

The PR response of confining layers:

In Fig. 1 a typical room temperature PR spectrum, in the region of the optical response of bulk InGaAs, is reported for the sample with a 60 nm thick LCL. The two PR features (labelled E_0^{HH} and E_0^{LH}) can be related, for their energy location [22], to transitions involving the split valence-bands in the partially-relaxed InGaAs CLs [23]. Arrows mark the transition energies, as derived from the best fit, from the heavy-hole (HH) and light-hole (LH) valence band maxima to the conduction band minimum of $In_{0.15}Ga_{0.85}As$. The broadening parameters Γ were 15 and 19 meV for HH- and LH- related transitions, respectively; the same broadening values were obtained for all the samples.

In order to discuss our experimental results, we briefly recall the effects of strain on the optical transitions of zinc-blende-type semiconductors [24,25].

Strained $In_xGa_{1-x}As$ grown on a (001)-oriented GaAs substrate is subject to a (001) biaxial stress, which can be decomposed into a hydrostatic and a [001] tensile uniaxial parts. The components ε_{ij} of the diagonal strain tensor are given by:

$$\varepsilon_{xx} = \varepsilon_{yy} = \varepsilon \qquad (2)$$

$$\varepsilon_{zz} = -(2C_{12}/C_{11})\,\varepsilon \qquad (3)$$

where z denotes the direction perpendicular to the interfaces, C_{ij} are the elastic stiffness constants and ε is the in-plane strain, which for $In_xGa_{1-x}As$ epitaxial layers is given by $\varepsilon = (a_0 - a_x)/a_x < 0$, where a_0 and a_x are the lattice parameters of GaAs and of free-standing $In_xGa_{1-x}As$, respectively. On the other hand, for epilayers exceeding the critical thickness t_C of the ternary alloy, strain relaxation occurs in mismatched layers via plastic deformation [13,26] and the residual strain ε_{res} is related to the in-plane lattice parameter $a_x^{\parallel}$ of the partially relaxed $In_xGa_{1-x}As$ layer by $\varepsilon_{res} = (a_x^{\parallel} - a_x)/a_x$, with $a_0 < a_x^{\parallel} < a_x$.

Concerning the E_0 optical transitions at $\mathbf{k} = 0$, the hydrostatic component of the compressive strain increases the energy gap between the topmost unsplit valence bands and the lowest lying conduction band. In addition, the uniaxial strain component splits the HH- and LH- valence bands. According to the deformation potential theory [24], the resulting energy gaps between the conduction and the split valence bands are:

$$E_0^{HH} = E_0 + \delta E_H - \delta E_S/2$$
$$E_0^{LH} = E_0 + \delta E_H + \delta E_S/2 - (\delta E_S)^2/(2\Delta_0) \qquad (4)$$

where E_0 and Δ_0 are the energy gap and the spin-orbit splitting of unstrained InGaAs and

$$\delta E_H = 2a\,\varepsilon\,(C_{11} - C_{12})/C_{11}, \qquad \delta E_S = 2b\,\varepsilon\,(C_{11} + 2C_{12})/C_{11} \qquad (5)$$

being *a* and *b* the hydrostatic and the shear deformation potentials, respectively. Thus, the valence band splitting

$$\Delta E = E_0^{LH} - E_0^{HH} , \quad (6)$$

as measured by the optical spectra, can be directly related to the strain ε of the layer.

The elastic constants, the deformation potentials and the spin-orbit splitting of the InGaAs alloys were obtained by linear interpolation between the end binary materials GaAs and InAs [27,22].

The E_0^{HH} and E_0^{LH} structures (see Fig. 1) were detected in all samples, at energies depending on the residual strain of CLs and, then, on the layer thickness. In Table I the energy E_0^{HH}, the valence band splitting ΔE and the corresponding in-plane residual strain ε_{res} of the partially relaxed $In_{0.15}Ga_{0.85}As$ LCLs are reported; the last parameter was determined all-optically from the measured valence bands splitting ΔE by using Eqs. (4-6), following the deformation potential theory for the partially-relaxed LCLs. As expected, the energies E_0^{HH} and ΔE decrease monotonically with increasing LCL thickness. The same behavior characterizes ε_{res}. For the composition x=0.15 the expected maximum strain of the $In_xGa_{1-x}As$ epilayer (pseudomorphic growth) is 1.063 % corresponding to a splitting ΔE of 65 meV, in good agreement with the measured value of 64 meV for the sample i1112 with LCL t = 20 nm (that is well below $t_C \approx$ 43 nm for $In_{0.15}Ga_{0.85}As$ on GaAs [13]).

In Fig. 2, the residual strain values of LCLs with thickness ranging from 20 to 360 nm are compared with the predictions of two different models on strain relaxation [13,26]. We note that the optically derived values of ε_{res} are in a very good agreement with that of the model of Marée *et al.* [13], which has been used to design the structures. In contrast, our results do not support the alternative model of Dunstan *et al.* [26].

PR measurements were performed also on samples without UCLs (not shown here). From the comparison of these spectra to the corresponding ones with UCLs negligible variations have been observed in the broadening parameter values of E_0^{HH} and E_0^{LH} transitions suggesting that UCLs are pseudomorphic to LCLs.

It is worth noting here that, according to Eqs. (4,5) the value of residual strain of CLs could be deduced by the shift of the energy gap $\Delta E_0 = E_0^{HH} - E_0$, which is linearly related to the strain; however, this approach would require the knowledge of E_0 as a function of x, with an accuracy of a few meV, which is generally not available [22,23]. This makes hard to distinguish among a few meV variations of the crucial quantity ΔE_0; thus we choose to use the more *clean* (and less composition dependent) information coming from the valence band splitting ΔE.

The ellipsometric results confirm the PR experimental findings. In Fig.3 we report the imaginary part ε_2 of the complex dielectric function of the $In_{0.15}Ga_{0.85}As$ LCLs, in the 2.5-3.5 eV interval, as derived from the analysis of the ellipsometric functions measured on samples without UCLs. The literature

dielectric function [28] of a bulk $In_{0.15}Ga_{0.85}As$ is reported for comparison. The ε_2 spectra are obtained from numerical inversion assuming the structural model of the sample and GaAs and InAs dielectric functions from literature. The QD plane was described as a layer of 3 ML equivalent thickness, corresponding to the InAs coverage; in fact, we verify the QD layer has no effect on ε_2 in this energy range. The behavior of ε_2 as a function of the LCL thickness obeys the predictions of strain effects on the interband dielectric function of ternary alloys [27,28]. The two clear peaks are related to the convolution of the E_1 and $E_1+\Delta_1$ interband critical point response. With decreasing the LCL thickness we note a blue-shift of the center of gravity of the E_1 and $E_1+\Delta_1$ peaks and an increase of the spin-orbit splitting Δ_1. In addition, the E_1 oscillator strength increases with respect to that of $E_1+\Delta_1$, as expected due to the reduced coupling between the states: these are clear fingerprints of an increasing strain along the growth direction [27]. These effects become more clear when considering the second-derivative spectrum of ε_2, that should be fitted with appropriate lineshapes: these and other results on the structures with UCLs are under investigation and will be the matter of future works.

The PR response of QDs:

In Fig. 4, the 90 K PR spectrum of InAs QDs embedded in an $In_{0.15}Ga_{0.85}As$ matrix (with a t=20 nm thick LCL) is compared to the spectrum of a similar structure with a GaAs matrix. In Fig. 5, instead, two InAs/$In_{0.15}Ga_{0.85}As$ structures with different LCL thickness (120 nm and 360 nm) are shown. In all samples the PR feature that dominates the spectrum is related to the ground-state transition (E_{gs}) of the main QD family [21]. Arrows mark the QD transition energies E_{gs} as derived from the best fit of the experimental features to a lineshape considering excitonic transitions in confined semiconductor systems (Eq. (1) with n =3).

A second weaker PR feature at higher energy (blue-shifted by 60-80 meV) was previously assigned to a second QD family and/or an excited state of the main family and will not be discussed here [21, 29, 30]. Nevertheless, for the analysis of the optical response of the main QD family the second QD PR feature was included in the fitting procedure to optimize the fits in order to obtain an accurate estimate of E_{gs} (see Table I).

We note that the broadening parameters of PR features related to the QD ensemble, due to dot size dispersion, are usually much larger than the bulk ones. The observed values of the broadenings range from 30 to 60 meV, so that the main PR feature and that due to a different QD family or an excited state of the main QD family overlap.

As introduced above, the QD PR features in the InAs/InGaAs structures exhibit a red-shift with respect to those of the InAs/GaAs ones. In Figs. 4 and 5 evidence is given of the two main contributions to this effect: *i)* the reduced QD-CL band discontinuities, due to the reduced band gap of the confining layer material and *ii)* the reduced QD strain, related to the reduced mismatch of QDs to LCLs. In fact, in the former case (Fig. 4), we compare the PR response of InAs QDs embedded in pseudomorphic InGaAs CLs grown on GaAs with that of similar dots embedded in a GaAs matrix. In both structures the strain field

experienced by the dots is the same, since the QDs are grown on LCLs that have the GaAs lattice parameter. Consequently, the red-shift of the E_{gs} energy is only related to the reduction of the carrier confining energies, due to the reduced (by ≈ 16%) band-discontinuities. On the other hand, in the second case (Fig. 5), we compare the PR response of two samples with InAs QDs embedded in $In_{0.15}Ga_{0.85}As$ matrices with LCLs of different thickness (t = 120 and 360 nm). In this case, the red-shift of the E_{gs} transition energy for the structure with thicker LCL is mainly due to the reduction of the QD strain, related to the lower mismatch of QDs to the LCL. Indeed, according to the model, for x=0.15 a variation of the LCL thickness from 120 nm to 360 nm results in a shift of E_g(InAs) (the energy band gap of the strained 3D InAs material) of 15 meV determined by the variation of the QD strain; the sum of band discontinuities instead and, then, that of carrier confinement energies are essentially unaffected.

Tuning the QD emission energy:

As aforementioned, one of the methods used to to tune the QDs emission of InAs QD nanostructures towards the 1.3 μm region is to embed the InAs nanoislands in InGaAs confining layers. In this approach, both the lowering of the QD-CL band discontinuities and the reduction of the QD strain contribute simultaneously to the red-shift of emission. In contrast, our approach is based on the concept of strain engineering of heterostructures, whereby the QD strain is designed *ad hoc*, by exploiting the thickness-dependent partial relaxation of LCLs with given compositions, as described by the Marée *et al.* theory [13]. Therefore, by means of our approach we are able to separately control the two aspects of the tuning mechanism that are related to the control of band discontinuities and of QD strain.

This aspect is evidenced in Fig. 6, where the experimental and the modeled dependences of E_{gs} on the LCL thickness t are compared in the 20-360 nm range. In the figure, E_g(InAs) is also reported. It should be noted that there is a considerable agreement of the experimental results to the model that can be used to design the structures.

From the PR and model data of Fig. 6 it can be seen that the sum of the band discontinuities, experimentally given by $\Delta E_g = E_0^{HH} - E_g(InAs)$, and that of carrier confining energies, $E_{conf} = E_{gs} - E_g(InAs)$ (which is corrected for the exciton binding energy), do not change significantly with the LCL thickness. Consequently, the variation of the energy gap E_g(InAs) of the QD material, due to the LCL-thickness-dependent strain imposed to the QDs, may be used for tuning the emission energy E_{gs} independently of the composition x of the CLs. Finally, it is worth noting that the accurate tuning of the QD emission wavelength obtained by simply varying the LCL thickness, when combined with a suitable choice of the composition x, opens the possibility of reaching interesting values, such as 1.3, 1.4, 1.5 μm [31]**.**

However, a few precautions must be taken in designing the structures for emission at given wavelengths, since In segregation and In-Ga interdiffusion [1,5-9] during growth and changes in the QD morphology induced by the reduction of strain [29, 32-35] may contribute to the red-shift. It should be noted that in our experiments the QD dimensions, as derived from AFM measurements on uncapped structures, are significantly independent on the QD strain and

modification of the nominal In concentration profiles in the structures should be drastically limited due to the low temperature (360 °C) used for the UCL growth process.

V. CONCLUSIONS

Photoreflectance measurements in the 0.8-1.5 eV energy range have been performed on ALMBE grown InAs/$In_{0.15}Ga_{0.85}As$ QDs structures with different lower confining layer thickness; the structures were designed to study the tuning mechanisms of the RT emission wavelength in spectral regions of optoelectronic interest and, in particular, in the 1.3 μm one. Spectral features related to InGaAs confining layers and to InAs QDs are clearly evidenced and analyzed according to lineshape model characteristic of modulation spectroscopy. The comparison of PR spectra of similar samples with and without UCL indicates that the optically-measured residual strain of the CLs is essentially the same and well agrees with the model for strain relaxation used to design the structures.

The experimental results on the QD-related transitions compare very favorably with the calculations performed by using a simple single-band, effective-mass-approximation model, when QD size parameters deduced by AFM measurements are used.

We prove that the effects of composition and thickness of the confining layers on the QD-CL barrier discontinuities and strain of QDs can be observed and singled-out by means of optical measurements on suitably designed structures and that these effects contribute separately to the red-shift of the ground state QD transition energies.

We can state that in our case the major role in determining the QD ground state energy is played by QD strain reduction. The experimental results confirm our model calculations whereby it can be concluded that by changing the CL thickness only the QD strain is affected, while the band discontinuities are unchanged. This proves the validity of our approach in tuning the emission energy of QDs by means of QD strain, simply controlled by varying the LCL thickness.

ACKNOWLEDGEMENTS

This work was partially supported by the MIUR-FIRB project "Nanotecnologie e nanodispositivi per la società dell'informazione". The authors would like to acknowledge M. Bertocchi for his valuable technical assistance.

References

[1] D. Bimberg, M. Grundmann and N. N. Ledentsov, *Quantum dot heterostructures*, Wiley, Chichester (1999).

[2] L. Seravalli, M. Minelli, P. Frigeri, P. Allegri, V. Avanzini, and S. Franchi, Appl. Phys. Lett. **82**, 2341 (2003)**.**

[3] M. Ustinov *et al.*, Appl. Phys. Lett. **74**, 2815 (1999).

[4] M. Ustinov *et al.*, Microelectronics Journal **31**, 1 (2000).

[5] Kenichi Nishi, Hideaki Saito, Shigeo Sugou, Jeong-Sik Lee, Appl. Phys. Lett. **74**, 1111 (1999).

[6] H.Y. Liu *et al.*, J. Appl. Phys. **88**, 3392 (2000).

[7] O. Dehaese, X. Wallart, and F. Mollot, Appl. Phys. Lett. **66**, 52 (1995).

[8] A. Bosacchi, F. Colonna, S. Franchi, P. Pascarella, P. Allegri and V. Avanzini, J. Cryst. Growth **150**, 185 (1995).

[9] P. B. Joyce, T. J. Krzyzewski, G. R. Bell, T. S. Jones, E. C. Le Ru, R. Murray, Phys. Rev. B **64**, 235317 (2001).

[10] D. E. Aspnes, Surf. Sci. **37**, 418 (1973).

[11] H. Shen, S.H. Panad, and F.H. Pollack, Phys. Rev. B **37**, 10919 (1988).

[12] J. Glembocki and B. Shanabrook, in *Semiconductors and Semimetals*, D.G. Seiler and C.L. Littler, Editors, Vol.36, p. 221, Academic Press, Boston (1992).

[13] P.M.J. Marée, J.C. Barbour, J.F. Van der Veen, K. L. Kavanagh, C. W. T. Bulle-Lieuvma, M.V.A. Viegers, J. Appl. Phys. **62**, 4413 (1987).

[14] A. Bosacchi, P. Frigeri, S. Franchi, P. Allegri, and V. Avanzini, J. Crystal Growth **175/176**, 771 (1997).

[15] A. Bosacchi, P. Frigeri, S. Franchi, P. Allegri, and V. Avanzini, J. Crystal Growth **201/202**, 1136 (1999).

[16] J.Y. Marzin and G. Bastard, Sol. Stat. Comm. **92**, 437 (1994)

[17] A.D. Andreev, J.R. Downes, D.A. Faux and E.P. O'Reilly, J. Appl. Phys. **86**, 297 (1999)

[18] L. Aigouy, T. Holden, F.H. Pollak, N.N. Ledentsov, W.M. Ustinov, P.S. Kop'ev, and D. Bimberg, Appl. Phys. Lett. **70**, 3329 (1997).

[19] F. H. Pollak, in *Handbook on Semiconductors*, P. Balkansky, Editor, Vol. 2, p. 527, North-Holland, Amsterdam (1994).

[20] G.L. Rowland, T.J.C. Hosea, S. Malik, D. Childs and R. Murray, Appl. Phys. Lett. **73**, 3268 (1998).

[21] M. Geddo, R. Ferrini, G. Guizzetti, M. Patrini, S. Franchi, P. Frigeri, G. Salviati, L. Lazzarini, Eur. Phys. J. B **16**, 19 (2000).

[22] S. Adachi, J. Appl. Phys. 53, 8775 (1982).

[23] *Properties of Lattice-matched and Strained Indium Gallium Arsenide*, P. Batthacharya, Editor, Chap. 9, p. 265, Inspec, London (1993).

[24] F. H. Pollak and M. Cardona, Phys. Rev. B **172**, 816 (1968).

[25] F. H. Pollak, in *Semiconductors and Semimetals*, T. P. Pearsall, Editor, Vol. 32, p. 17, Academic, London (1990).

[26] D. J. Dunstan, P. Kidd, L. K. Howard, R. P. Dixon, Appl. Phys. Lett. **59**, 3390 (1991).

[27] L.C. Andreani, D. De Nova, S. Di Lernia, M. Geddo, G. Guizzetti, and M. Patrini, C. Bocchi, A. Bosacchi, C. Ferrari and S. Franchi, J. Appl. Phys. **78**, 6745 (1995), and references therein.
[28] C. Pickering, R.T. Carline, M.T. Enemy, N.S. Garawal and L.K. Howard, Appl. Phys. Lett. **60**, 2412 (1992).
[29] M. Geddo, G. Guizzetti, M. Patrini, R. Pezzuto, S. Franchi, P. Frigeri, G. Trevisi, in *Semiconductor Quantum Dots*, S. Fafard, R. Leon, D. Huffaker, R. Noetzel, Editors, Vol. 642, J3.7.1, Materials Research Society, Warrendale, Pennsylvania (2001).
[30] M. Galluppi, M. Capizzi, F. Boscherini, M. Catalano, A. Passaseo, R. Cingolani, P. Frigeri, S. Franchi, *Proc. of the 25th Int. Conf. on the Physics of Semiconductors*, N. Miura and T. Ando, Editors, p. 1199, Springer, Berlin (2001).
[31] L. Seravalli, P. Frigeri, M. Minelli and S. Franchi, *to be published*.
[32] B. Lita, R.S. Goldman, J.D. Phillips, P.K. Bhattacharya, Appl. Phys. Lett. **75**, 2797 (1999).
[33] N.-T. Yeh, T.-E. Nee, J.-I. Chyl, T.M. Hsu and C.C. Huang, Appl. Phys. Lett. **76**, 567 (2000).
[34] T. Yamauchi, Y. Matsuba, Y. Ohyama, M. Tabuchi, and A. Nakamura, Jpn. J. Appl. Phys. **40**, 2069 (2001).
[35] M.V. Maximov *et al.*, Phys. Rev. B **62**, 16671 (2000).

TABLE I: Energy gap (**E_0^{HH}**), valence band splitting (ΔE) and optically-determined in-plane strain values (ε_{res}) of the partially relaxed $In_{0.15}Ga_{0.85}As$ LCLs of different thickness, grown on GaAs. The UCL thickness is 20 nm for all structures. The corresponding ground-state transition energies E_{gs} of QDs are also reported.

Sample	**LCL t** (nm)	**E_0^{HH}** (eV) 300 K	**E_0^{HH}** (eV) 90 K	**ΔE** (meV) 300 K	**ε_{res}** %	**E_{gs}** (eV) 90 K
i1112	20	1.280	1.355	64	1.048	1.024
i1111	60	1.277	1.352	59	0.955	1.018
i1092	120	1.241	1.314	39	0.609	0.998
i1091	220	1.217	1.292	26	0.398	0.983
i1100	360	1.213	1.289	24	0.366	0.973

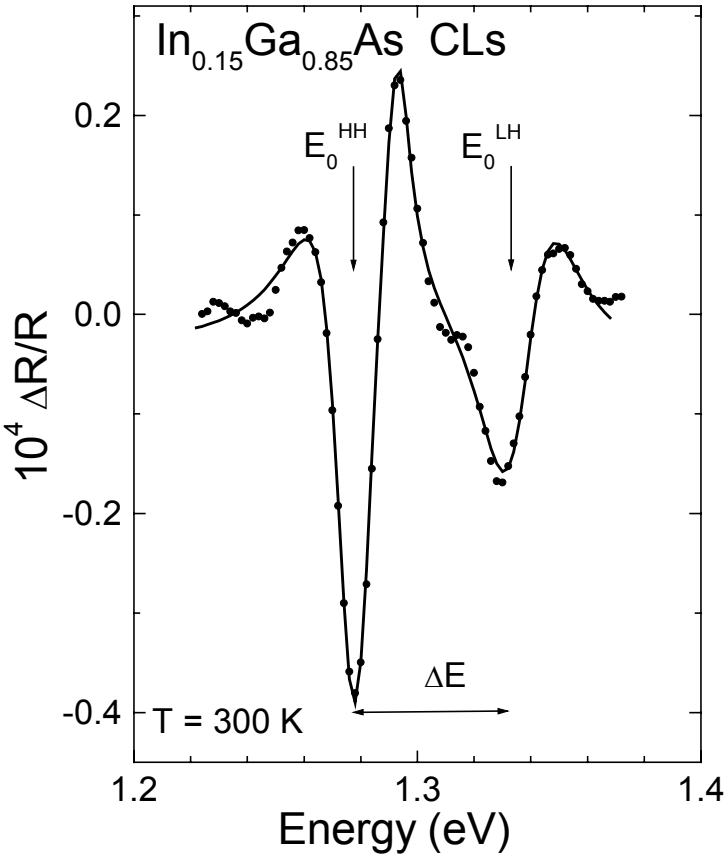

Figure 1: Room temperature PR spectrum of a InAs/ $In_{0.15}Ga_{0.85}As$ QD structure with a partially-relaxed LCL (t = 60 nm); the spectrum displays the splitting ΔE of the InGaAs HH and LH valence bands. Arrows mark the transition energies as derived from the best fit to the experimental features.

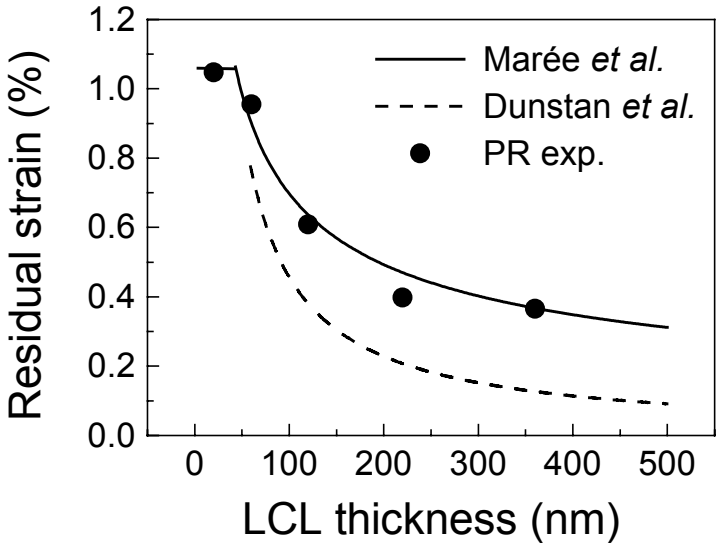

Figure 2: Comparison of the optically-determined residual strain (dots) for InAs/ $In_{0.15}Ga_{0.85}As$ structures with different LCL thickness to the results of models (lines) proposed in Refs. [13,26].

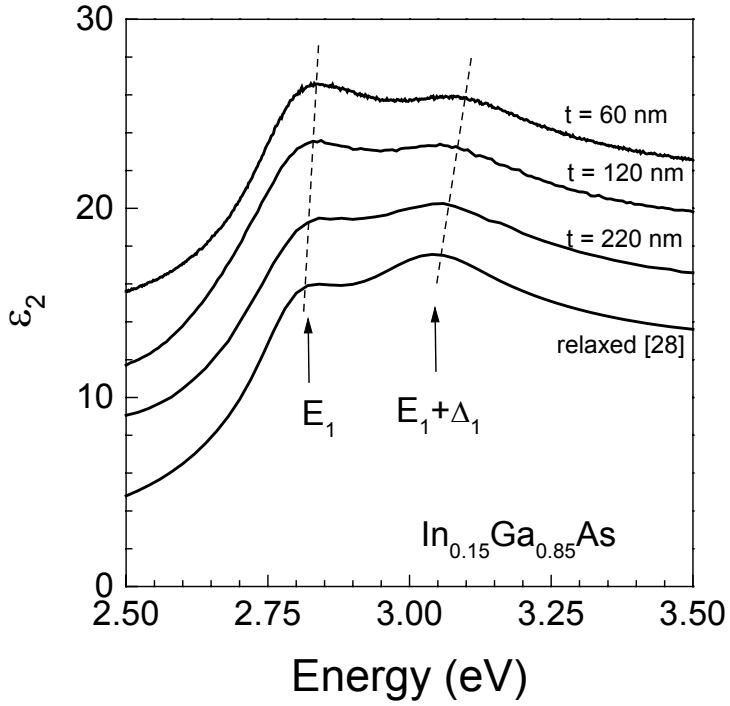

Figure 3: Imaginary part of the complex dielectric function of InAs/$In_{0.15}Ga_{0.85}As$ structures with different LCL thickness and of fully-relaxed $In_{0.15}Ga_{0.85}As$ [28] in the interband spectral region. The curves are shifted by a constant value for clarity.

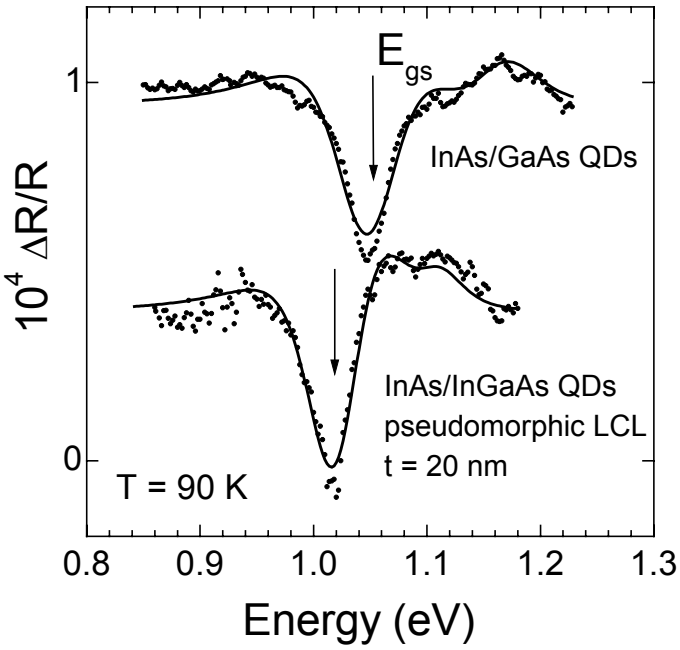

Figure 4: PR response at 90 K of InAs QD ground-state transition E_{gs} highlighting the red-shift in a InAs/$In_{0.15}Ga_{0.85}As$ structure on a pseudomorphic LCL with respect to a InAs/GaAs one; the red-shift is due to the different band discontinuities. The curves are shifted vertically for clarity.

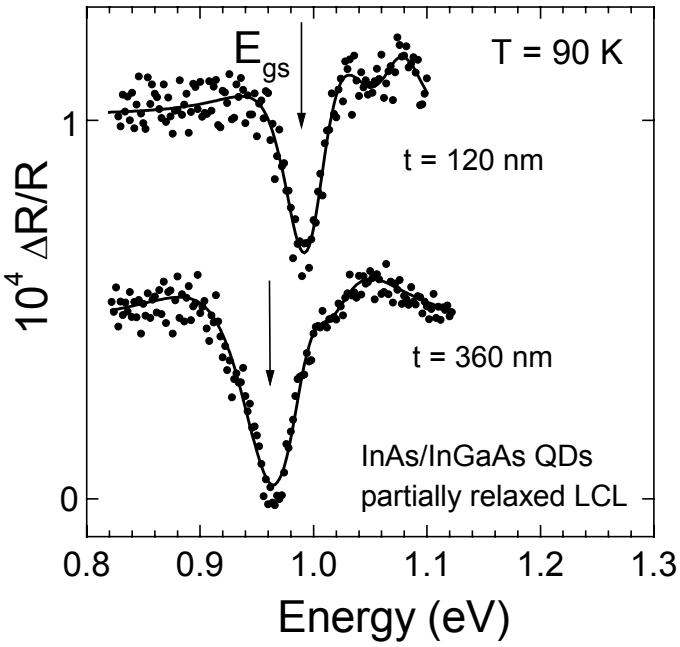

Figure 5: PR response at 90 K of InAs QD ground-state transition E_{gs} showing the red-shift in the InAs/$In_{0.15}Ga_{0.85}As$ structures with different LCL thickness t, as due to the different QD strain. The curves are shifted vertically.

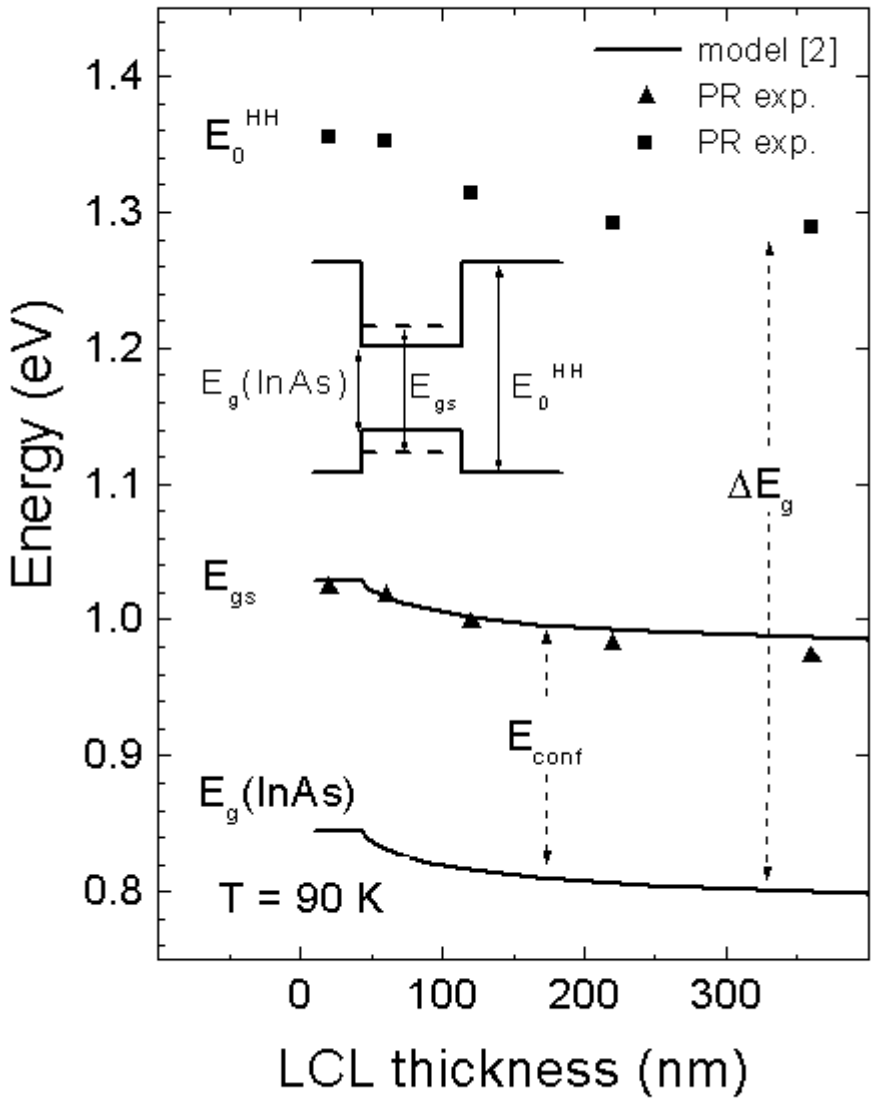

Figure 6: Comparison of the behavior of QD ground-state transition E_{gs} versus LCL thickness, as obtained by PR measurements (symbols) and by the model calculations proposed in Ref. [2] (line). The measured LCL energy gap E_0^{HH} and the calculated energy gap E_g(InAs) are also reported. ΔE_g and E_{conf} indicate the sum of the band discontinuities and the sum of the carrier confining energies (corrected for the exciton binding energy).